Hue University Journal of Science: Natural Science
Vol. 129, No. 1D, 5–13, 2020

pISSN 1859-1388
eISSN 2615-9678

FABRICATION AND CHARACTERIZATION OF SOME PHYSICAL PROPERTIES OF PZT–PMnN–PSbN CERAMICS DOPED WITH ZnO

Nguyen Truong Tho[1,*], Le Dai Vuong[2]

[1] University of Sciences, Hue University, 77 Nguyen Hue St., Hue, Vietnam
[2] Faculty of Chemical and Environmental Engineering, Hue Industrial College, Hue city, Vietnam

* Correspondence to Nguyen Truong Tho <ntthokh@hueuni.edu.vn>

(Received: 12 April 2020; Accepted: 21 April 2020)

Abstract. The effect of the ZnO addition in pure perovskite PZT–PMnN–PSbN ceramics sintered from 950 to 1200°C has been investigated. The phase structure of ceramics changes from rhombohedral to tetragonal and the temperature decreases with the increase of the ZnO content. The limitation of Zn^{2+} concentration for the solubility in PZT–PMnN–PSbN systems is about 0.25% wt., at which the ceramic shows some good physical properties such as the density of 8.20 g/cm^3, some dielectric constants including ε_r = 1,555 and ε_{max} = 32,900. The highest value of ε_{max} about 22,000 was found at 1 kHz at the temperature of T_m around 575 K. Using an extended Curie–Weiss law the diffuse phase transition was determined. Cole–Cole analyses showed the non–Debye type relaxation in the system.

Keywords: Perovskite, ceramics, PZT–PMnN–PSbN, diffuse phase transition, Cole–Cole analyses

1 Introduction

Last several decades have extensive study on the relaxor ferroelectrics since their discovery by Smolenskii *et al.* [1], owing to their significant technical importance on the application of electromechanical devices such as multilayer ceramic capacitors, electrostrictive transducers, micro–displacement positioners. Recently, there have been studies on lead-free ferroelectric materials to overcome lead toxicity. [2–5] However, their physical properties have not good enought to replace the role of Pb in ferroelectric materials. [6–12] Therefore, in addition to continuing research on lead-free ferroelectric materials, further improvement of the physical properties of Pb related materials have been necessary.

As $Pb(Mn_{1/3}Nb_{2/3})O_3$ (PMnN), $Pb(Sn_{1/3}Nb_{2/3})O_3$ (PZN) is a member of lead–based relaxor ferroelectric family with different cations on the *B*–site of perovskite lattice. They are ferroelectric materials have characteristics as high dielectric constant, the temperature at the phase transition point between the ferroelectric and paraelectric phase are broad (the diffuse phase transition) and a strong frequency dependency of the dielectric properties. So far, the sintering temperature of PZT–based ceramics is usually too high, approximately 1200°C [13–16]. In order to reduce the sintering temperature at which satisfactory densification could be obtained, various material processing methods such as the 2–stage calcination method [17], high energy mill [18] and liquid phase sintering [15–**17**, 19–21] have been performed. Among these methods, liquid phase sintering is basically an effective method for aiding densification of specimens at low sintering temperature.

Perovskite based relaxor ferroelectric materials have generated considerable interest due to rich diversity of their physical properties and possible applications in various technologies like memory storage devices, micro-electro-mechanical systems, multilayer ceramic capacitors and recently, in the area of opto-electronic devices [14–16]. It occupies a particular place among the complex oxides $A(B'_mB''_{1-m})O_3$ with promising dielectric properties. In contrast to the normal ferroelectrics, they exhibit a strong frequency dispersion of the dielectric constant without the change in crystalline phase structure in the temperature region near T_m (the temperature, at which the diffuse permittivity is given maximum). Basically in compositionally homogenous systems, the quenched random disorder causes a breaking the long-range polar order in the unit cell level, leading to broad the $\varepsilon'(T)$ [17]. Such materials exhibit a slow enough relaxation dynamics and hence have been termed the ferroelectric relaxor [17,18]. Burns and Decol [19] have observed an existence of polar-regions in the relaxor at temperatures higher than Tm. In principle, the relaxors are classified in two families: The first is the lead manganese niobate (PMN) 1:2 family such as $Pb(Mg_{1/3}Nb_{2/3})O_3$, and the second is the lead scandium niobate (PSN) 1:1 family such as $Pb(Sc_{1/2}Nb_{1/2})O_3$.

In PZT–$Pb(Mg_{1/3}Nb_{2/3})O_3$ and PZT–$Pb(Zn_{1/3}Nb_{2/3})O_3$ systems, belong to the first family, PT–$Pb(Sc_{1/2}Nb_{1/2})O_3$, belongs to the second family, the dielectric transition complied with the extended Curie-Weiss law. The results of study in these systems indicate that the dielectric relaxation to be non-Debye type [20,26].

In this study, we investigated the effect of ZnO addition on the sintering behavior and physical properties of the PZT–PMnN–PSbN ceramics. we report results of our studies on the dielectric behavior of PZT–PMnN–PSbN +x% wt. ZnO ceramics which are given by the combination of a normal ferroelectric with two above relaxor families. The real and imaginary parts of the dielectric permittivity and loss dielectric in a frequency range of (0.1–500kHz) at a temperature range of (270–320^{o}C) has been analyzed. We have investigated the diffuse phase transition of the system by using the extended Curie – Weiss law and determined the parameters in this relation by fitting.

2 Experimental procedure

2.1 Samples preparation

PZT–PMnN–PSbN + x% wt. ZnO ceramics were prepared from reagent grade raw material oxides via the Columbite and Wolframite method in order to suppress the formation of pyrochlore phase. The processing of synthezise was through three steps:

Step 1: Synthezise $MnNb_2O_6$ and $Sb_2Nb_2O_8$; $MnCO_3$ and Nb_2O_5; Sb_2O_3 and Nb_2O_5 were mixed and acetone- milled for 20 h in a zirconia ball mill and then calcined at 1250^{o}C for 3 h to form $MnNb_2O_6$ and $Sb_2Nb_2O_8$. The material was acetone-ground for 10 h in the mill and dried again.

Step 2: Synthezise PZT–PMnN–PSbN calcined powders

Reagent grades PbO, ZrO_2, TiO_2 were mixed with $MnNb_2O_6$ and $Sb_2Nb_2O_8$ powders by ball mill for 20 h in acetone. The mixed powders were dried and calcined at 850^{o}C for 2 h and then the calcined powders were ground by ball mill in acetone for 24 h.

Step 3: Synthezise PZT–PMnN–PSbN + x% wt. ZnO ceramics

The PZT–PMnN–PSbN calcined powders were mixed with x % wt. ZnO, x = 0.05, 0.15, 0.2, 0.25, 0.30, 0.40, 0.50 symbols for Z05, Z10, Z15, Z20, Z25, Z30, Z40, Z50, respesively, and acetone-milled for 8 h in the zirconia ball mill and then dried.

pISSN 1859-1388
eISSN 2615-9678

The ground materials were pressed into disk 12mm in diameter and 1.5mm in thick under 100MPa. The samples were sintered at 850, 900, 950, 1000 and 1050°C for 3 h in an alumina crucible to form the ZnO doped PZT–PMnN–PSbN ceramics. The sintered and annealed samples were ground and cut to 1mm in thick. A silver electrode was fired at 500°C for 10 minutes on the major surfaces of samples. Poling was done in the direction of thickness in a silicon oil bath under 30kV/cm for 15 minutes at 120°C.

2.2 Microstructure, dielectric properties measurement

The bulk densities of sintered specimens were measured by Archimedes technique. The crystalline phase was analyzed using an *X*-ray diffactometer (XRD). The microstructure of the sintered bodies was examined using a scanning electron microscope (SEM). The grain size was measured by using the line intercept method. The dielectric permittivity and dielectric dissipation of samples were measured by the highly automatized RLC HIOKI 3532 at 1 kHz.

3 Results and discussion

3.1 Effect of ZnO addition on the sintering behavior of PZT – PMnN – PSbN ceramics

Fig. 1 shows the variations of density of PZT–PMnN–PSbN + *x*% wt. ZnO samples at different sintering temperature. It can be seen that the densities of PZT–PMnN–PSbN ceramics change as functions of sintering temperature and the content of ZnO sintering aid. Without ZnO addition, it is seen that sufficient densification occurs at temperatures 1250°C, while ZnO added ceramic samples exhibit densification at a temperature as low as 950°C (the density of 8.20 g/cm^3 at ZnO content of 0.25% wt.), indicating that ZnO is quite useful to lower sintering temperature of ceramics, similarly to reports on ZnO added PZT-based ceramics [14–16]. When the amount of ZnO increase from 0 to 0.25% wt., the density of samples increases with the increasing amount of ZnO and the sintering temperature and then decreases.

.

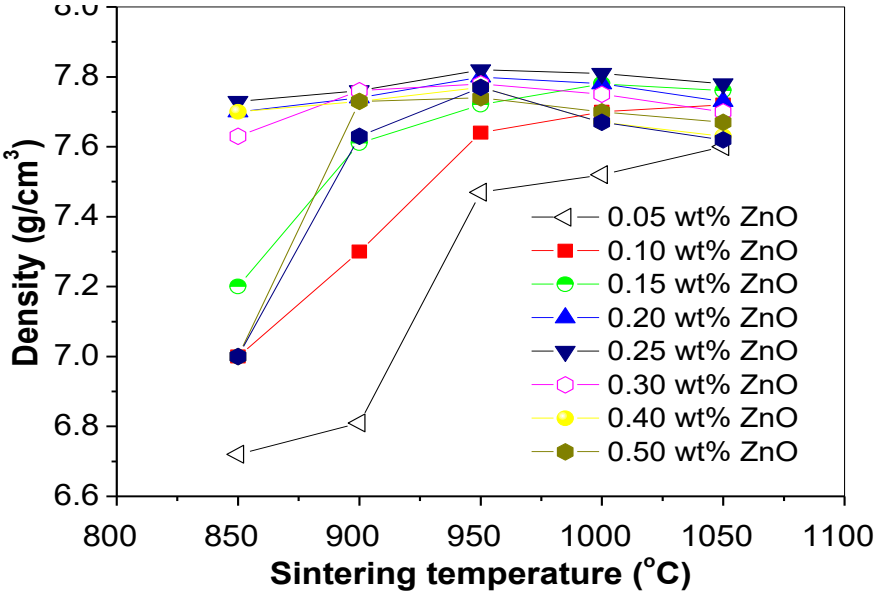

Fig. 1. Density of the PZT–PMnN–PSbN +x% wt. ZnO ceramicsas a function of sintering temperature

According to the above results, the optimized sintering temperature of the ZnO doped PZT–PMnN–PSbN ceramics is 950^{0}C. So, the addition of ZnO improved the sinterability of the samples and caused an increase in the density at low sintering temperature

3.2 Effect of ZnO addition on the structure, microstructure of PZT–PMnN–PSN ceramics

Fig. 2 shows X-ray diffraction patterns (XRD) of the PZT–PMnN–PSbN ceramics at the different contents of ZnO. All samples have pure perovskite phase, the phase structure of ceramics changes from rhombohedral to tetragonal with the increase of the ZnO content.

Fig. 3 shows SEM micrographs of fractured surface of ZnO added PZT–PMnN–PSbN specimens sintered at 950^{0}C for 2 h. The sintering aid added PZT–PMnN–PSbN specimens showed uniform and densified structure. In the ZnO added PZT–PMnN–PSbN systems, the low-temperature sintering mechanism primarily originated from transition liquid phase sintering. In the early and middle stages of sintering process, ZnO additives with a low melting point forms a liquid phase, which wets and covers the surface of grains, and facilitates the dissolution and migration of the species.

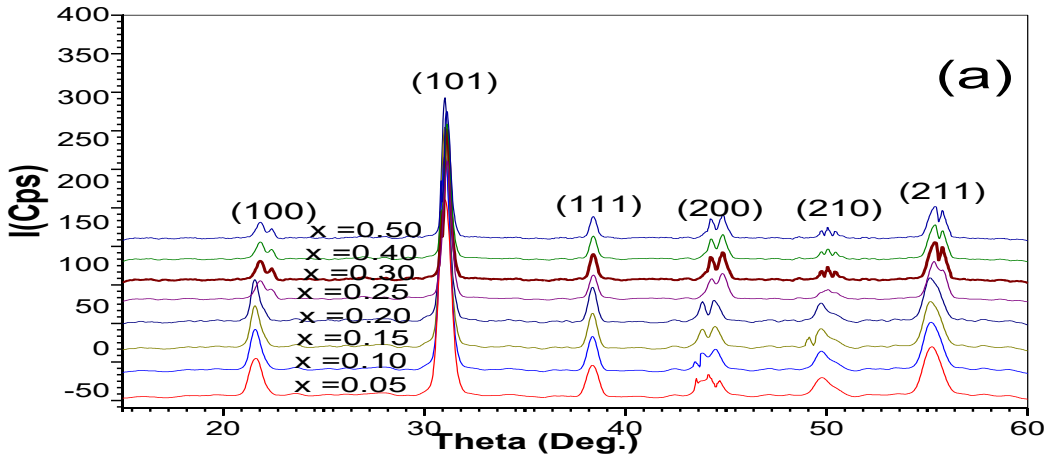

Fig. 2. X-ray diffraction patterns of ceramics with different ZnO contents

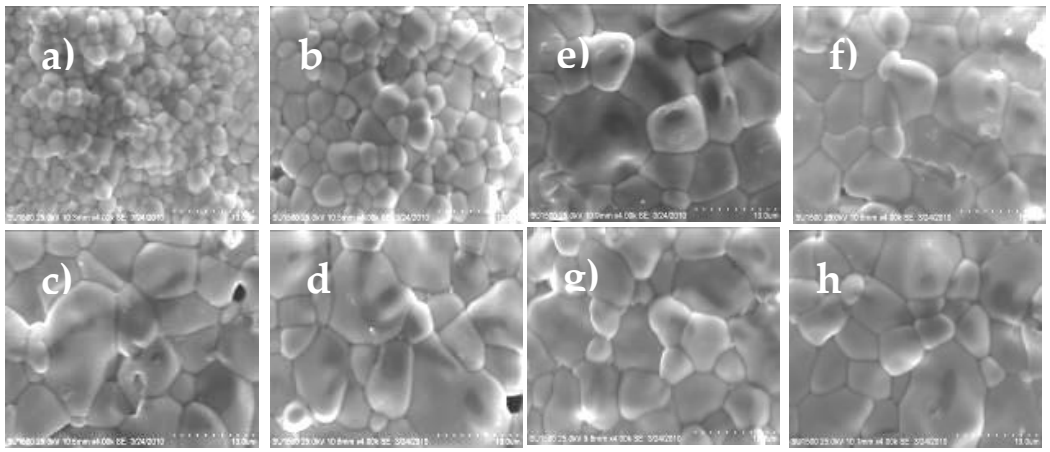

Fig. 3. SEM micrographs of fractured surface of PZT–PMnN–PSbN specimens with different amounts of ZnO additive: a) 0.05 % wt., b) 0.1 % wt., c) 0.15 % wt., d) 0.2 % wt., e) 0.25 % wt., f) 0.3 % wt., g) 0.4% wt. and 0.5 % wt.

pISSN 1859-1388
eISSN 2615-9678

3.3 Effect of ZnO addition on the diffuse phase transition of PZT–PMnN–PSbN system

Fig. 4 presents the temperature dependence of real (ε') and imaginary (ε'') parts of dielectric constant and loss tangent (tanδ) of PZT–PMnN–PSbN ceramics at 1 kHz. The dielectric permittivity maximum (ε'_{max}) and its temperature (T_m), are listed in Table 1. As seen in Fig. 4, the dielectric properties exhibited characteristics of a relaxor material in which the phase transition temperature occurs within a broad temperature range. This is one of the characteristics of ferroelectrics with disordered perovskite structure [23]. The origin of disorder is caused by variation in local electric field, variation in local strain field and formation of vacancies in the crystalline structure of materials. A random local electric field resulting from the different valences of *B*–site cations and a variation of the local strain field due to the difference in radius of *B*–site cation [24]. For PZT–PMnN–PSbN system, the *B*–site is occupied by Zn^{2+}, Mn^{2+}, Sb^{3+}, Nb^{5+}, Zr^{4+} and Ti^{4+}. Thus, the degree of disorder in this system is mainly caused by the difference of valences of Zn^{2+} with Zr^{4+}/Ti^{4+}.

The value of T_m decrease with increasing of ZnO content while that of ε′max is of maximum at Z25 (0.25% wt. ZnO). This may be explained that the Curie temperature reflects the stability of *B*–site ions in the oxygen octahedron, which can be determined by the formation energy of octahedra. Therefore, the substitution of *B*–site Zr^{4+} or Ti^{4+} ion with Zn^{2+} can decrease the stability of the B-site ions in the octahedra.

It was observed that the temperature T_m of maximum permittivity of all samples shifted to higher temperatures while ε_{max} decreased and $(tan\delta)_{max}$ increased upon increasing frequency. Fig.4 also showed that all samples have a diffuse phase transition in the transition temperature region.

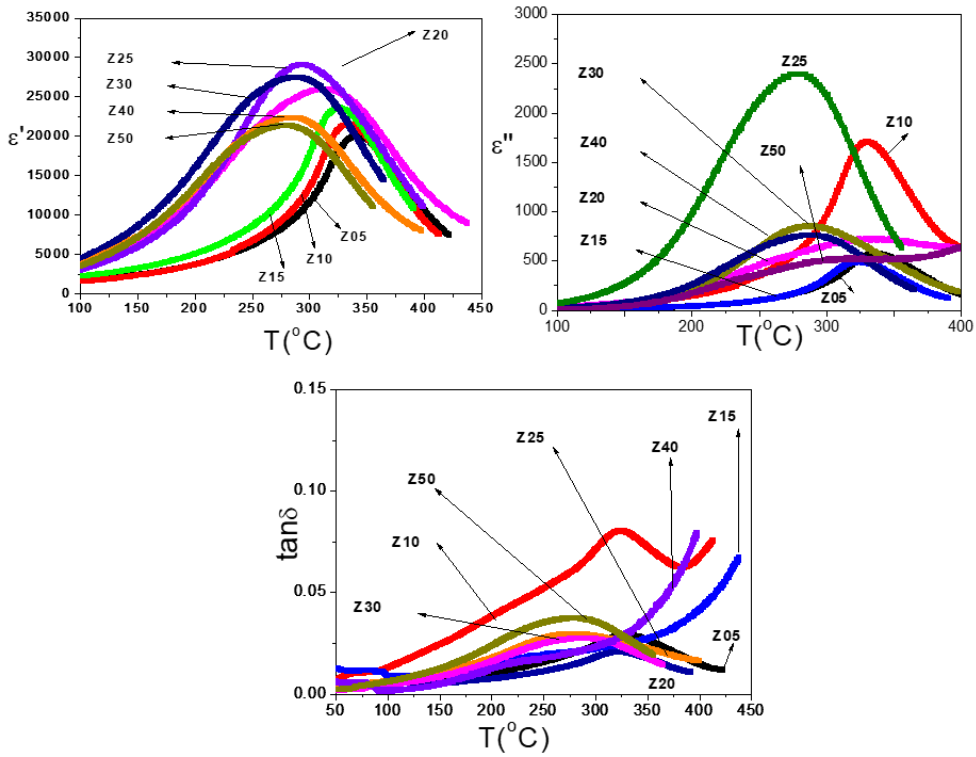

Fig. 4. The temperature dependence of real (ε′), imaginary (ε′′) parts of dielectric constant and loss tangent (tanδ) of PZT-PMnN-PSbN + x % wt. ZnO ceramics at 1 kHz

The real (ε') and imaginary (ε'') parts of dielectric constant and loss tangent ($tan\delta$) can be calculated from the measured capacitance and phase values of the samples versus temperature. The maximum dielectric permittivity (ε'_{max}) at 1kHz, its temperature (T_m), and the fitting parameters using the modified Curie–Weiss law are listed in Table 1. The value of T_m increases with increasing of PMnN component, but the ε'max abnormally depends on ZnO component and has the maximum value as x = 0.25.

In order to examine the diffuse phase transition and relaxor properties, the following modified Curie–Weiss formula has been used for analyzing of experimental data:

$$\frac{1}{\varepsilon} - \frac{1}{\varepsilon_{max}} = \frac{(T-T_m)^{\gamma}}{C'} \quad (1)$$

or

$$log\left(\frac{1}{\varepsilon} - \frac{1}{\varepsilon_{max}}\right) = \gamma log(T - T_m) - logC' \quad (2)$$

where C′ is the modified Curie–Weiss constant, and γ is the diffuseness exponent, which changes from 1 to 2 for normal ferroelectrics to fully disorder relaxor ferroelectrics, respectively. Eq. (1) can be solved graphically using a log-log plot, as shown in Fig. 2.

The given value of γ at 1 kHz as presented in Table 1 is an evidence to suggest the diffuse phase transition (DPT) happened in the samples. It is expected that the disorder in the cation distribution (compositional fluctuations) causes the DPT where the local Curie points of different micro-regions are statistically distributed in a wide temperature range around the mean Curie point. The non-equality of phase transition temperature obtained from $\varepsilon(T)$ and $tan\delta(T)$ measurement also confirms the existence of the DPT. It has shown that the value of the diffuseness, γ, increases with increasing of ZnO component. This indicates that, the disorder in B site in materials increases with increasing of ZnO component in the systems.

A common characteristic of all relaxors is the existence of disorder in crystalline structure. In principle the disorder is caused by variation in local electric field as well as in local strain field related to the formation of vacancies in the crystalline structure of materials and/or with the different valences and radius of *B*–site cation [20]. For PZT–PMnN–PSbN system, the *B*-site is occupied by Mn^{2+}, Sb^{3+}, Nb^{5+}, Zr^{4+} and Ti^{4+}. Both of Mn^{2+} and Sb^{3+} have the ionic radii rather similar: Mn^{2+} (0.08nm), Sb^{3+} (0.082nm), as substituted on Nb^{5+} (0.069nm), Zr^{4+} (0.079nm) or Ti^{4+} (0.068nm) and Zn^{2+} (0.099nm) [21]. Thus, the degree of disorder in this system is mainly caused by the difference of valences of Zn^{2+}, Mn^{2+} and Sb^{3+} with Zr^{4+}/Ti^{4+}.

Table 1. The dielectric permittivity maximum (ε'_{max}) and its temperature (T_m), and the fitting parameters to the modified Curie–Weiss law.

Sample	ε	tan δ	ε'max	T_m (K)	γ	C'×105 (K)	T_B (K)
Z05	1220	0.03	16054	533	1.4432	3.673	576
Z10	1370	0.03	19066	546	1.4567	4.563	588
Z15	1520	0.03	24085	555	1.4345	5.123	596
Z20	1537	0.01	24488	557	1.5237	4.433	609
Z25	1655	0.006	32900	575	1.7989	6.793	614
Z30	1262	0.007	22789	579	1.8922	6.993	618
Z40	1001	0.012	18848	581	1.9241	5.773	620
Z50	990	0.010	16541	582	1.9878	3.993	628

pISSN 1859-1388
eISSN 2615-9678

Fig.6. presents a Curie-Weiss dependence $1/\varepsilon'$ of the Z25 sample. It is clearly seen that at the temperature region far above T_m the dependence fitted well to a linear line. It is supposed to be related with an appearance of the paraelectric phase in the sample. The linear line has cut the $1/\varepsilon(T)$ curve at a point called as Burns temperature T_B, the temperature at which the disorder nanoclusters start to appear with cooling down the sample. The values T_B given from fitting are also presented in Table 1. The obtained results suggested that in the diffuse phase transition materials the ferroelectric disorder nanoclusters could exist in a temperature region much higher than the T_C evaluated from Curie-Weiss relationship.

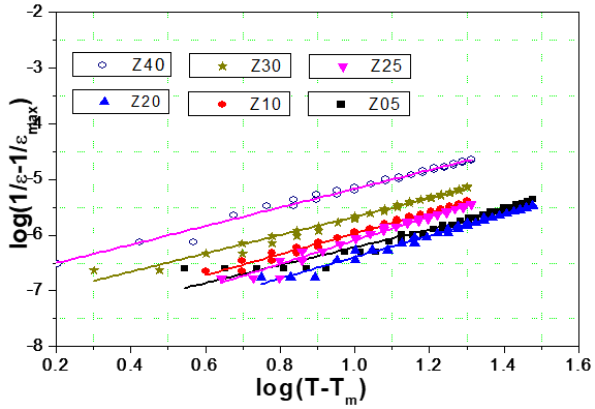

Fig. 5. Dependence of log(1/ε–1/εmax) on log(T – Tm) for Z25 sample at 1 kHz

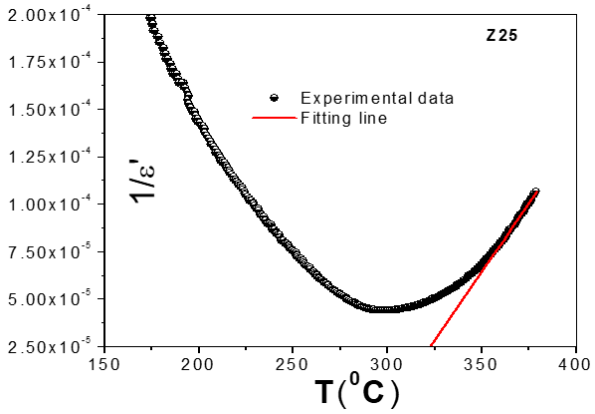

Fig. 6. Curie-Weiss dependence of the permittivity of the Z25 sample at temperature much higher than Tm

3.4 Cole-Cole diagrams

Complex dielectric constant formalism is the most commonly used experimental technique to analyze dynamics of the ionic movement in solids. Contribution of various microscopic elements such as grain, grain boundary and interfaces to total dielectric response in polycrystalline solids can be identified by the reference to an equivalent circuit, which contains a series of array and/or parallel RC element [20].

To study the contribution originated from difference effects, Cole-Cole analyses have been made at difference temperatures.

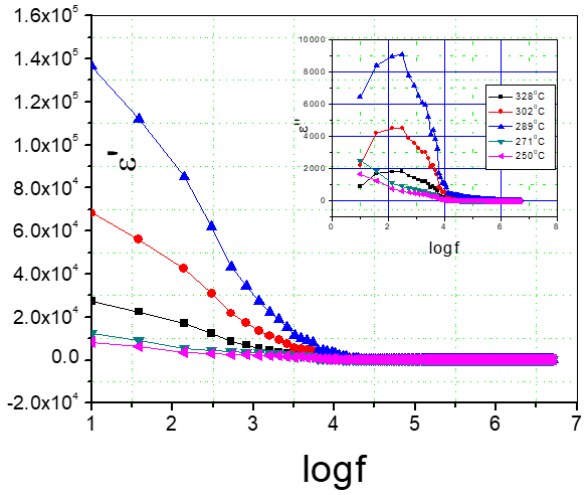

Fig. 7. The frequency dependence of real and imaginary parts of dielectric permitivity of Z25 sample at different temperatures

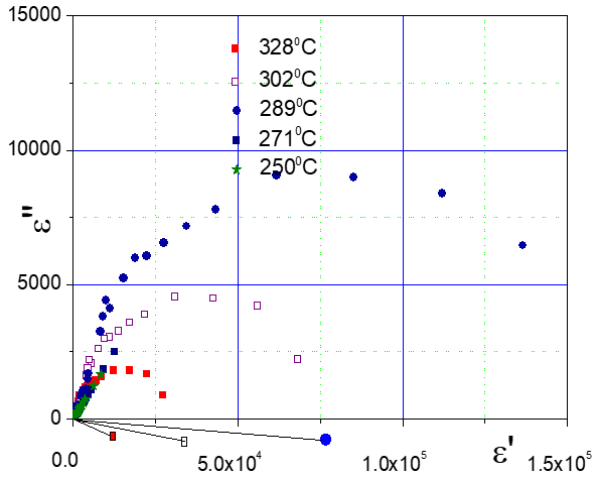

Fig. 8. Cole-Cole diagrams of Z25 sample at different temperatures

It was observed that the dielectric constant data at low temperature, i.e., up to about 289°C, did not take the shape of a semicircle in the Cole-Cole plot and rather showed the straight line with large slope, suggesting the insulating behaviour of the compound at low temperature. It could further be seen that with the increase in temperature, the slope of the lines decreased towards the real (ε') axis and at temperature above 289°C, a semicircle could be traced (Fig. 8).

The Cole-Cole plot also provides the information about the nature of the dielectric relaxation in the systems. For polydispersive relaxation, the plots are close to circular arcs with end points on the axis of real and the centre below this axis. The complex dielectric constant in such situations is known to be described by the empirical relation:

$$\varepsilon^* = \varepsilon' - i\varepsilon'' = \varepsilon_\infty + \frac{\varepsilon_S - \varepsilon_\infty}{1+(i\omega\tau)^{1-\alpha}} \quad (3)$$

where εs and ε∞ are the low- and high–frequency values of ε, α is a measure of the distribution of relaxation times. The parameter α can be determined from the location of the centre of the Cole-Cole circles, of which only an arc lies above the ε'-axis [22]. It is evident from the plots that the relaxation process differs from monodispersive Debye process (for which α = 0). The parameter α, as determined from the angle subtended by the radius of the circle with the ε′- axis passing through the origin of the ε″-axis [23–25], shows a slight increase in the interval [0.233, 0.187, 0.196] with the decrease of temperature from 601K to 562K, implying a slight increase in the distribution of the relaxation time with decreasing temperature below Tm.

4 Conclusions

Effect of ZnO addition on the sintering behavior and dielectric properties of 0.9Pb($Zr_{0.49}Ti_{0.51}$)O_3–0.07Pb($Mn_{1/3}Nb_{2/3}$)O_3–0.03Pb($Sb_{1/2}Nb_{1/2}$)O_3 eramics were investigated. The addition of ZnO improved the sinterability of the samples and caused an increase in the density and grain size at low sintering temperature (950°C). Analysis of the microstructure evolution showed that the solubility limit of Zn ions in PZT–PMnN–PSbN systems was about 0.25 % wt.. At the ZnO content of 0.25% wt., dielectric properties of ceramics are best: the density of 8.20 g/cm^3, the the dielectric constant, ε_r = 1655, ε_{max} = 32900, the dielectric loss (tanδ) of 0.006. All samples have pure perovskite phase, the phase structure of ceramics changes from rhombohedral to tetragonal with the increase of the ZnO content. All the samples exhibit the relaxor behaviour with diffuse phase transition with modeling of the dielectric data using modified Curie–Weiss law. The Cole–Cole plot also provides the information about the nature of the dielectric relaxation in the systems.

References

1. Smolenskii GA, Isupov VA, Agranovskaya AI. New Ferroelectrics of Complex Composition of the Type $A_2^{+2}(B_I^{3+}B_{II}^{5+})O_6$. Sov Phys Solid State. 1959;1:150-151.
2. Inoue A, Nguyen TT, Noda M, Okuyama M. Low Temperature Preparation of Bismuth-Related Ferroelectrics by Hydrothermal Synthesis. Proc 2007 16th IEEE Inter Symp Applica Ferroe. 2007;136-137.
3. Nguyen TT, Kanashima T, Okuyama M. Leakage Current Reduction and Ferroelectric Property of $BiFe_{1-x}Co_xO_3$ Thin Films Prepared by Chemical Solution Deposition Using Rapid Thermal Annealing. MRS online Proc. 2011; 1199:1199-F06-19.
4. Tho NT, Inoue A, Noda M, Okuyama M, Low Temperature Preparation of Bismuth-Related Ferroelectrics Powder and Thin Films by Hydrothermal Synthesis. IEEE Trans Ultrasonic Ferroelec Freq Control. 2007; 54:2603-2607.
5. Truong-Tho N, Vuong LD. Effect of Sintering Temperature on the Dielectric, Ferroelectric and Energy storage properties of SnO_2-doped $Bi_{0.5}(Na_{0.8}K_{0.2})_{0.5}TiO_3$ Lead-free Ceramics. J Adv Dielectric [Internet]. 2020.

pISSN 1859-1388
eISSN 2615-9678

6. Truong-Tho N, Nghi-Nhan NT. Fabrication by Annealing at Approximately 1030°C and Electrical Characterization of Lead-Free (1-x)$Bi_{0.5}K_{0.5}TiO_3$–$x$$Ba(Fe_{0.5}Nb_{0.5})_{0.05}Ti_{0.95}O_3$ Piezoelectric Ceramics. J Electronic Mater. 2017;46: 3585-3591.

7. Vuong LD, Tho NT. The Sintering bahavior and Physical properties of Li_2CO_3-Doped $Bi_{0.5}(Na_{0.8}K_{0.2})_{0.5}TiO_3$ Lead-Free Ceramics. Inter J Mater Res. 2017; 108(3): -222-227.

8. Vuong LD, Truong-Tho N. Effect of ZnO Nanoparticles on the Sintering Behavior and Physical Properties of $Bi_{0.5}(Na_{0.8}K_{0.2})_{0.5}TiO_3$ Lead-Free Ceramics. J Electronic Mater. 2017;46:6395-6402.

9. Tho NT, Kanashima T, Sohgawa M, Ricinschi D, Noda M, Okuyama M. Ferroelectric Properties of $Bi_{1.1}Fe_{1-x}Co_xO_3$ Thin Films Prepared by Chemical Solution Deposition Using Iterative Rapid Thermal Annealing in N_2 and O_2. Jpn J Appl Phys. 2010; 49:09MB05-7.

10. Tho NT, Kanashima T, Sohgawa M, Ricinschi D, Noda M, Okuyama M. Ferroelectric Properties of $Bi_{1.1}Fe_{1-x}Co_xO_3$ Thin Films Prepared by Chemical Solution Deposition Using Iterative Rapid Thermal Annealing in N_2 and O_2. Jpn J Appl Phys. 2010; 49: 09MB05-7.

11. Tho NT, Kanashima T, Okuyama M. Leakage Current Reduction and Ferroelectric Property of $BiFe_{1-x}Co_xO_3$ Thin Films Prepared by Chemical Solution Deposition Using Iterative Rapid Thermal Annealing at Approximately 520°C. Jpn J Appl Phys. 2010;49:095803-6.

12. Leontsev SO, Eitel RE. Dielectric and Piezoelectric Properties in Mn-Modified (1−x)$BiFeO_3$–x$BaTiO_3$ Ceramics. J American Ceram Soc. 2009;92:2957-2961.

13. Luo W, Wang D, Liu T, Cai J, Zhang L, Liu Y. Room Temperature Simutaneously Enhanced Magnetization and Electric Polarization in $BiFeO_3$ Ceramics Synthesized by Magnetic Annealing. Appl Phys Lett . 2009;94:202507-3.

14. Gao F, Cheng L, Hong R, Liu J, Wang C, Tian C. Crystal Structure and Piezoelectric Properties of $x$$Pb(Mn_{1/3}Nb_{2/3})O_3$–(0.2 − x)$Pb(Zn_{1/3}Nb_{2/3})O_3$–0.8$Pb(Zr_{0.52}Ti_{0.48})O_3$ Ceramics. Ceram Inter. 2009;35:1719-1723.

15. Vuong LD, Gio PD, Tho NT, Chuong TV. Relaxor Ferroelectric Properties of PZT-PZN-PMnN Ceramics. Indian J Eng Mater Sci. 2013;20:555-560.

16. Luan NDT, Vuong LD, Chuong TV, Tho NT. Structure and Physical Properties of PZT-PMnN-PSN Ceramics near the Morphological Phase Boundary. Adv Mater Sci Eng. 2014; 2014:1-8.

17. Tsai CC, Hong CS, Shih CC, Chu SY. Electrical Properties and Temperature Behavior of ZnO-Doped PZT–PMnN Modified Piezoelectric Ceramics and Their Applications on Therapeutic Transducers. J Alloy Comp. 2012;511:54-62.

18. Vuong LD, Gio PD. Effect of Li_2CO_3 Addition on the Sintering Behavior and Physical Properties of PZT-PZN-PMnN Ceramics. Inter J Mater Sci Appl. 2013;2(3):89-93.

19. Burns G, Dacol FH. Glassy Polarization Behavior in Ferroelectric Compounds $Pb(Mg_{1/3}Nb_{2/3})O_3$ and $Pb(Zn_{1/3}Nb_{2/3})O_3$. Solid Stat Comm [Internet]. 1983; 48(10):853-856.

20. Chen J, Chan HM, Harmer MP. Ordering Structure and Dielectric Properties of Undoped and La/Na-Doped $Pb(Mg_{1/3}Nb_{2/3})O_3$. J Ame Ceram Soc. 1989;72(5):593-598.

21. Cole KS, Cole RH. Dispersion and Absorption in Dielectrics I. Alternating Current Characteristics. J Chem Phys. 1941;9:341-351.

22. Barranco AP, Abreu YG, Noda RL. Dielectric Relaxation and Conductivity Behavior in Modified Lead Titanate Ferroelectric Ceramics. J Phys Condense Matter. 2008;20(50):1-10.

23. Setter N, Cross LE. The role of B-site cation disorder in diffuse phase transition behavior of perovskite ferroelectrics. J Appl Phys. 1980;51:4356-4360.

24. Randall CA, Bhalla AS. Nanostructural-Property Relations in Complex Lead Perovskites. Jpn J Appl. 1990; 29(2):327-333.

25. He X, Zeng X, Zheng X, Qiu P, Cheng W, Ding A. Fabrication and characteristics of relaxor ferroelectric PZN-PZT (53/47) thin films by a MOD process. J Phys: Conf Seri. 2008;152:1-5.

26. Pirc R, Blinc R. Vogel-Fulcher. Freezing in Relaxor Ferroelectrics. Phys Rev B. 2007;76:020101-3.